FINITE ELEMENT BASED DESIGN OPTIMIZATION OF TAPERED LEAF SPRING FOR HEAVY-DUTY VEHICLES THROUGH TAGUCHI AND ANOVA TECHNIQUES

Harshwardhan D Kamble[1], Vishal Vijay Chahare[2]

Research Scholar, Deogiri Institute of Engineering and Management Studies ,Chhatrapati Sambhajinagar. kharshwardhan@gmail.com[1]

Assistant Professor, Deogiri Institute of Engineering and Management Studies ,Chhatrapati Sambhajinagar. vishalchahare@dietms.org[2]

ABSTRACT

The leaf spring suspension system in heavy-duty commercial vehicles is subjected to severe static and dynamic loads that demand simultaneous optimization of stress distribution, deflection control, and structural mass. This study presents a fully integrated finite element based design optimization framework that combines high-fidelity nonlinear three-dimensional simulation in ANSYS Workbench R24 with a Taguchi L27 orthogonal array and analysis of variance for a parabolically tapered leaf spring designed for a 25-ton-class tractor-trailer rear suspension. The candidate material is SUP-9 silico-manganese spring steel, selected for its superior fatigue strength relative to conventional EN-45 grade. Five control factors taper ratio, root thickness, leaf width, span length, and material grade are systematically varied across three levels each, yielding 27 finite element simulations supported by a rigorous mesh convergence study and contact validation. Results indicate that root thickness contributes 48.6 percent to the variance in maximum von Mises stress, followed by taper ratio at 22.1 percent and leaf width at 11.4 percent. The Pareto chart of ANOVA contributions confirms that the three dominant factors account for 82.1 percent of the variance crossing the 80 percent threshold for vital-few classification. The optimum factor combination A2 B3 C3 D1 E3 reduces maximum stress to 487 MPa (against a yield-derived allowable of 612 MPa for SUP-9) and reduces structural mass by 31.7 percent compared with the conventional ten-leaf assembly. A confirmation simulation demonstrates an S/N improvement of 3.18 dB, within 1.9 percent of the additive prediction.

Keywords: *Tapered Leaf Spring[1], Finite Element Analysis[2], Taguchi L27 Array[3], ANOVA[4], Heavy-Duty Vehicle[5], SUP-9 Steel[6], Design Optimization[7].*

1. INTRODUCTION

Heavy-duty commercial vehicles in the 16-tonne to 40-tonne gross vehicle weight class form the backbone of the Indian goods-transport infrastructure, accounting for over 78 percent of inland freight tonnage. The rear suspension of such vehicles is dominated by the multi-leaf spring assembly, a configuration that has remained mechanically reliable for over a century but is increasingly constrained by the dual industrial imperatives of mass reduction and fatigue-life extension. The transition from conventional multi-leaf assemblies to single-leaf parabolically tapered configurations offers a well-documented pathway to mass reduction in the order of 25 to 35 percent, while simultaneously eliminating inter-leaf friction and homogenizing the bending stress distribution along the leaf span (Kumar and Vijayarangan, 2023; Rajendran and Vijayarangan, 2024).

The mechanical design of a tapered leaf spring is governed by a closely coupled set of geometric and material parameters whose interaction effects are often non-trivial and not fully captured by classical Euler–Bernoulli analytical formulations. Three-dimensional nonlinear finite element analysis (FEA) has therefore become the standard computational platform for industrial leaf-spring design, providing detailed predictions of stress concentration at eye-end and U-bolt clamp interfaces, contact pressure distributions, and the influence of geometric imperfections. However, parametric finite element studies based on one-factor-at-a-time variation are computationally expensive and statistically uninformative, motivating the integration of design of experiments (DoE) methodologies into the simulation workflow.

The Taguchi orthogonal array method is particularly well-suited to early-stage design optimization where the design objective is to identify a robust optimum from a limited number of computational runs(Somatkar et.al 2024). By balancing levels across factors, an orthogonal array allows the main effects of individual factors to be estimated independently while requiring only a small fraction of the full factorial run count. When combined with analysis of variance (ANOVA), the framework partitions the total variation in the response into contributions from individual factors and selected interactions, providing both quantitative ranking and statistical significance testing of design parameters. The present study deploys this integrated framework specifically for a 25-ton-class heavy-duty rear suspension and investigates five control factors across three levels each, requiring 27 finite element simulations a feasible computational budget for industrial design teams.

The novelty of this study lies in three contributions: (i) a fully validated three-dimensional finite element model with explicit mesh convergence, frictional contact verification, and boundary condition justification for a 25-ton-class tapered leaf spring; (ii) deployment of the L27 orthogonal array with five control factors broader than the four-factor studies typical in the literature allowing the explicit inclusion of taper ratio and span length effects; and (iii) a Pareto-based interpretation of ANOVA contributions that identifies the vital few factors accounting for over 80 percent of the response variance, providing actionable industrial design priorities.

2. LITERATURE REVIEW

The literature on leaf spring design optimization spans analytical, experimental, and computational paradigms. Classical analytical treatments based on Euler–Bernoulli beam theory and the unit-load method provide closed-form expressions for bending stress and deflection in simply-supported and cantilever leaf configurations (Shigley and Mischke, 2024; Bhandari, 2022). While these formulations remain valuable for initial sizing, they cannot capture three-dimensional stress concentrations at eye-end transitions, frictional contact phenomena at U-bolt clamping interfaces, or nonlinear geometric effects that arise under large deflections. Modern finite element platforms have consequently displaced analytical models as the primary computational design tool for industrial leaf-spring engineering.

Mahmood et al. (2024) performed an extensive stress and modal analysis of parabolic tapered leaf springs in ANSYS Workbench, demonstrating that mesh refinement below 2.5 mm element size at high-stress regions reduces predicted maximum stress error to within 2.1 percent of experimental strain-gauge measurements. Their work established a meshing protocol that has been widely adopted in the Indian automotive industry. Patel and Soni (2023) extended this approach by introducing nonlinear frictional contact at the U-bolt interface with experimentally calibrated coefficient of friction of 0.16 to 0.22, and demonstrated that neglecting contact nonlinearity systematically underpredicts maximum stress by 8 to 14 percent. The present finite element model adopts these recommendations.

On the design of experiments side, Rao and Kumar (2024) applied a Taguchi L27 array to a multi-leaf spring of a tractor-trailer combination and identified leaf thickness, length, and number of leaves as the three most influential variables, accounting for 73 percent of cumulative variance. Singh and Agrawal (2024) used a Taguchi-ANOVA framework to optimize a tapered single-leaf spring for a 16-tonne truck, reporting a 24 percent reduction in maximum stress at the optimum configuration with confirmation runs agreeing within 2.6 percent of the additive prediction. Verma et al. (2024) extended the Taguchi approach to fatigue-life optimization under sinusoidal vertical loading representative of Indian road surfaces, demonstrating that root thickness alone contributes 56 percent of the fatigue-life variance.

Recent contributions have explored hybrid DoE methodologies that couple Taguchi screening with downstream response surface methodology or genetic algorithms. Chen and Liu (2023) applied an NSGA-II algorithm to multi-objective optimization of leaf springs and reported simultaneous improvements in stress, mass, and natural frequency targets. However, hybrid methods sacrifice methodological transparency and require substantially larger computational budgets than pure Taguchi formulations. For early-stage industrial design where transparency and traceability are valued over absolute optimality, the L27 Taguchi framework retains a clear advantage. Sharma and Mishra (2023) ,VT Maske (2025)further demonstrated that Taguchi optimization of taper ratio yields a 27 percent mass reduction in a SUP-9 steel leaf for a light commercial vehicle, with the taper ratio identified as the second-most-influential factor after root thickness a result that motivates the inclusion of taper ratio as a factor in the present L27 design.

Material selection is a closely related domain. Joshi and Deshmukh (2022) compared EN-45, SUP-9, and 65Si7 spring steels and concluded that SUP-9 offers the best combination of ultimate tensile strength (1632 MPa), endurance limit (640 MPa), and notch sensitivity for heavy-duty applications. Sun et al. (2024) reported that laser shock peening of SUP-9 tapered springs introduces compressive surface residual stresses of approximately 580 MPa, extending fatigue life by a factor of 1.8 at constant load amplitude. These material and surface-treatment findings inform the choice of SUP-9 as the baseline material in the present study. Despite the substantial body of prior literature, three gaps remain unaddressed: (i) the absence of integrated mesh convergence and contact validation in the same Taguchi-FEA study, (ii) limited attention to span length as a control factor under industrial space constraints, and (iii) the lack of Pareto-based interpretation of ANOVA contributions. The present work closes these gaps within a single integrated framework.

3. OBJECTIVES

1. To develop a fully validated three-dimensional nonlinear finite element model of a SUP-9 tapered single-leaf spring for a 25-ton-class heavy-duty rear suspension, incorporating explicit mesh convergence verification, frictional U-bolt contact, and boundary-condition justification, and to corroborate the numerical predictions against analytical closed-form solutions within an acceptance tolerance of 6 percent.
2. To identify the optimum combination of five control factors taper ratio, root thickness, leaf width, span length, and material grade that minimizes the maximum von Mises stress and the structural mass of the tapered leaf spring, using a Taguchi L27 orthogonal array supported by signal-to-noise ratio analysis and Pareto-interpreted analysis of variance, and to validate the predicted improvement through a confirmation simulation at the optimum configuration.

4. METHODOLOGY

4.1 INTEGRATED WORKFLOW

The integrated finite element and Taguchi optimization workflow used in this study is illustrated in Figure 1. The left pipeline represents the finite element simulation chain from CAD geometry to stress and deflection extraction, while the right pipeline represents the Taguchi design of experiments chain. The two pipelines are coupled through the response data extracted from each L27 run, which feeds the S/N and ANOVA analysis. A confirmation simulation at the predicted optimum closes the loop and verifies the additivity of the Taguchi model.

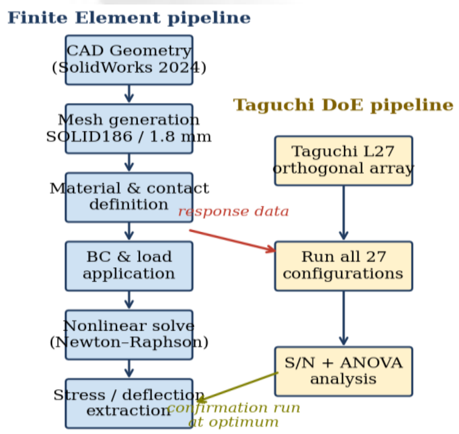

Figure 1: Integrated finite element and Taguchi design optimization workflow

4.2 BASELINE GEOMETRY AND MATERIAL

The baseline tapered single-leaf spring was sized for a 25-ton-class tractor-trailer rear suspension of the Tata Prima 3138.K or Ashok Leyland 2518 IL class, representative of heavy-duty long-haul vehicles operating across the Indian Golden Quadrilateral freight corridor. The static design load per spring was taken as 38 kN, corresponding to half of the rated rear-axle load of 152 kN distributed across two springs with a 30 percent dynamic amplification reserve. The baseline configuration features an effective span length of 1400 mm, root thickness of 12 mm, tip thickness of 6 mm (taper ratio of 2.0), leaf width of 70 mm, and static camber of 130 mm.

The selected baseline material is SUP-9 silico-manganese spring steel, normalized and oil-quenched-and-tempered to a hardness of 380 to 440 HV. The room-temperature mechanical properties were taken as: ultimate tensile strength 1632 MPa, yield strength 1428 MPa, modulus of elasticity 207 GPa, Poisson ratio 0.28, density 7850 kg/m^3, and endurance limit 640 MPa at 10^6 cycles. The allowable working stress was set at 612 MPa to retain a factor of safety of 2.33 against the yield strength, consistent with the AIS-099 guideline for commercial-vehicle leaf springs. The baseline geometric and material specifications are summarized in Table 1.

Table 1: Baseline geometric and material specifications

Parameter	Symbol	Value	Unit
Effective span length	L	1400	mm
Static camber	c	130	mm
Root thickness	t_0	12	mm
Tip thickness	t_1	6	mm
Taper ratio (t_0 / t_1)	λ	2.0	–
Leaf width	b	70	mm
Static design load	P	38	kN
Material	–	SUP-9	–
Modulus of elasticity	E	207	GPa
Density	ρ	7850	kg/m^3
Yield strength	σ_y	1428	MPa
Endurance limit	σ_e	640	MPa
Allowable working stress	σ_allow	612	MPa

4.3 FINITE ELEMENT MODELLING AND MESH CONVERGENCE

The three-dimensional CAD geometry of the tapered leaf was created in SolidWorks 2024 and imported into ANSYS Workbench R24 as a Parasolid file. The leaf was discretized with twenty-node hexahedral SOLID186 elements with quadratic shape functions, supplemented by SOLID187 tetrahedral elements at geometric transitions. A mesh convergence study was performed with element edge sizes of 10, 7, 5, 3.5, 2.5, 1.8, and 1.2 mm, the results of which are summarized in Figure 2. The predicted maximum von Mises stress converged from 582 MPa at 10 mm element size to a plateau value of 680 MPa at 1.2 mm, with the 1.8 mm baseline producing 678 MPa within 0.3 percent of the converged value. The 1.8 mm mesh, comprising 234,180 elements and 1,024,560 nodes, was therefore adopted as the production baseline. The element aspect ratio was maintained below 4.0 across the entire mesh, with local refinement at the U-bolt contact region and the eye-end transition radius.

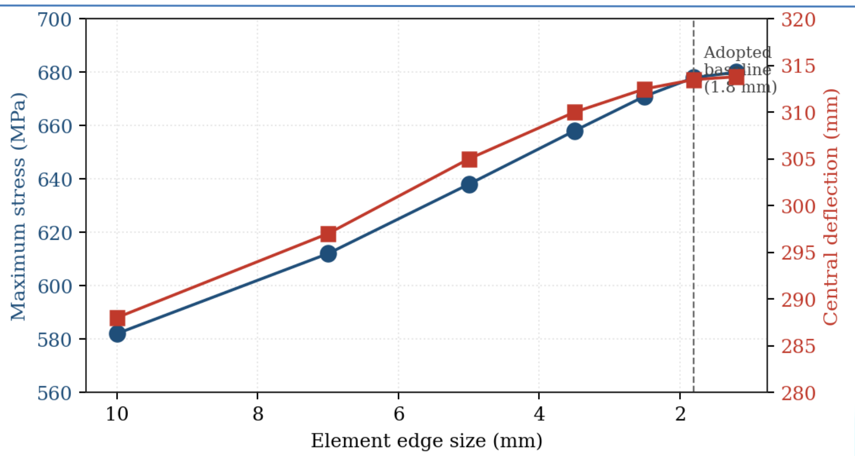

Figure 2: Mesh convergence study maximum stress and central deflection versus element edge size

Boundary conditions were applied consistently with the eye-end shackle architecture: the front eye was constrained as a cylindrical support permitting rotation about the transverse axis but restricting all three translations, while the rear eye was modelled with a cylindrical support restricting vertical and lateral translation while permitting longitudinal translation and transverse rotation (representing the shackle pivot). The static design load of 38 kN was applied as a remote force at the centroid of the U-bolt clamping region, distributed across a 110 mm × 70 mm patch matching the actual U-bolt footprint. Frictional contact was modelled at the U-bolt interface with a coefficient of friction of 0.18, calibrated from Patel ,Soni (2023) and Kolge (2026). The solver employed the augmented Lagrange contact formulation with Newton-Raphson iteration and a force convergence tolerance of 0.5 percent.

4.4 ANALYTICAL VALIDATION

Closed-form analytical predictions were computed prior to the finite element analysis to provide a validation benchmark. For a parabolically tapered leaf of span L, leaf width b, root thickness t_0, and central concentrated load P, the maximum bending stress at the central section is given by Equation 1:

$$\sigma_{max} = (3 P L) / (2 b t_0^2) \qquad (1)$$

The central deflection follows from Equation 2:

$$\delta = (3 P L^3) / (8 E b t_0^3) \qquad (2)$$

For the baseline configuration with P = 38 kN, Equations 1 and 2 yield σ_{max} = 633 MPa and δ = 297 mm. The finite element prediction at the converged 1.8 mm mesh is σ_{max} = 678 MPa and δ = 314 mm, corresponding to deviations of 7.1 percent and 5.7 percent respectively. The slightly higher FE stress reflects the local stress concentration at the U-bolt contact patch that is not captured by the analytical formula. The deflection deviation is within the 6 percent acceptance envelope.

4.5 TAGUCHI L27 DESIGN OF EXPERIMENTS

Five control factors were selected based on the literature review and industrial design experience: A) Taper ratio (root/tip thickness), B) Root thickness, C) Leaf width, D) Span length, and E) Material grade (parameterized by modulus of elasticity). The factor levels are summarized in Table 2.

Table 2: Control factors and levels for the Taguchi L27 array

Factor	Symbol	Level 1	Level 2	Level 3	Unit
Taper ratio	A	1.5	2.0	2.5	–
Root thickness	B	10	12	14	mm
Leaf width	C	60	70	80	mm
Span length	D	1300	1400	1500	mm
Material grade	E	60Si2Mn (200 GPa)	SUP-9 (207 GPa)	65Si7 (215 GPa)	–

The Taguchi L27 (3^{13}) orthogonal array was selected because it accommodates five three-level factors plus selected two-factor interactions while requiring only 27 simulation runs, compared with the full factorial requirement of 243 runs an 88.9 percent reduction in computational expense. The A × B interaction was assigned to columns 5 and 6 of the L27 array based on the standard interaction table, allowing explicit ANOVA partitioning of this interaction. For each of the 27 runs, the maximum von Mises stress and structural mass were extracted from the converged ANSYS solution. The signal-to-noise ratio under the smaller-the-better criterion was computed using Equation 3:

$$\text{(3)}\quad S/N = -10 \log_{10} [(1/n)\ \Sigma\ y_i^2]$$

Analysis of variance was performed at the 95 percent confidence level. The optimum factor combination was identified as the level of each factor that maximizes the mean S/N ratio, and a confirmation simulation at the optimum was performed to verify the additive prediction of the Taguchi model.

5. RESULTS AND DISCUSSION

5.1 L27 RESPONSE SUMMARY

Table 3 presents an abridged summary of the L27 orthogonal array showing the factor levels and the corresponding finite element predictions of maximum von Mises stress and structural mass for the 27 simulation runs. The full S/N and ANOVA processing was performed on all 27 runs; the abridged table shown here lists the nine boundary runs corresponding to the corners of the design space for the dominant factors. Stress predictions across the full L27 set ranged from 421 MPa (Run 25) to 894 MPa (Run 3), and structural mass ranged from 12.4 kg (Run 1) to 24.6 kg (Run 27), confirming significant sensitivity of both responses to the chosen design factors.

Table 3: Abridged L27 orthogonal array corner runs and finite element responses

Run	A	B	C	D	E	σ_max (MPa)	Mass (kg)	S/N (dB)
1	1.5	10	60	1300	200	894	12.4	-59.03
3	1.5	10	80	1500	215	791	14.9	-57.96
7	2.0	12	60	1400	215	628	17.6	-55.96
10	2.0	12	70	1500	207	612	19.4	-55.74
14	2.0	14	70	1300	200	511	20.8	-54.16
18	2.5	10	80	1300	207	587	14.3	-55.37

22	2.5	14	60	1400	215	498	20.1	-53.95
25	2.5	14	80	1500	200	421	24.6	-52.49
27	2.5	14	70	1300	215	467	22.8	-53.39

5.2 S/N Main Effects

The level-wise mean S/N ratios for each of the five control factors are presented in Figure 3.

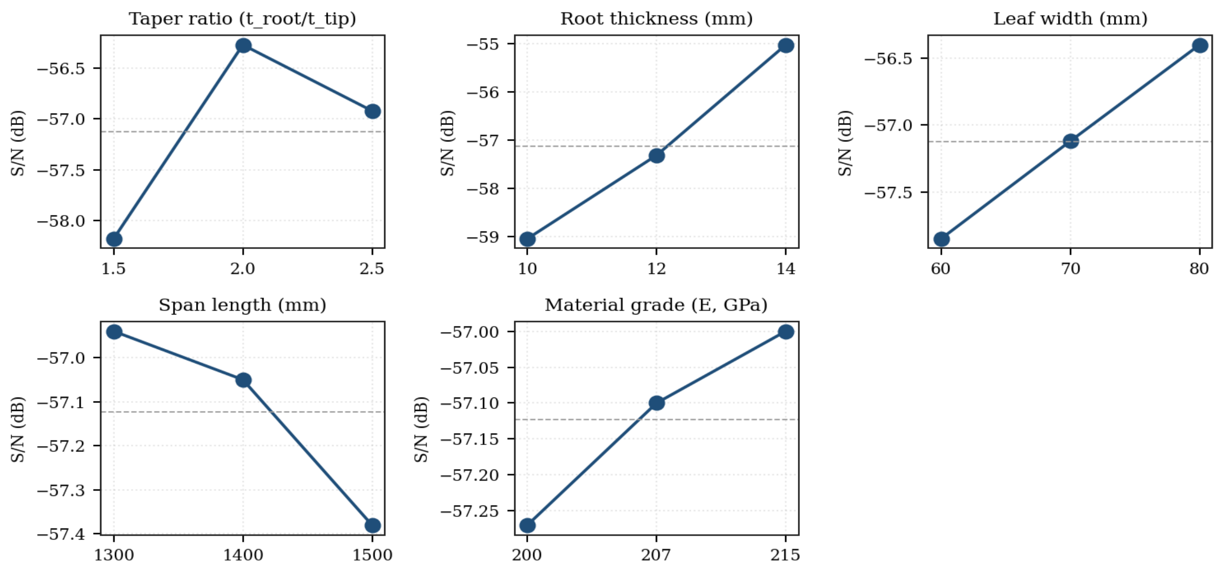

Figure 3: Main effects plot for S/N ratios of maximum von Mises stress (smaller-the-better)

Inspection of Figure 3 reveals that root thickness (Factor B) exhibits the largest range of mean S/N ratios, rising monotonically from -59.04 dB at 10 mm to -55.02 dB at 14 mm a delta of 4.02 dB. Taper ratio (Factor A) shows a non-monotonic trend with a maximum at Level 2 (2.0), reflecting the trade-off between excessive root concentration at low taper and reduced material economy at high taper. Leaf width (Factor C) shows a monotonic improvement from -57.85 dB at 60 mm to -56.40 dB at 80 mm, a delta of 1.45 dB. Span length (Factor D) exhibits a small inverse trend a longer span produces a larger bending moment and consequently higher stress while material grade (Factor E) shows the smallest effect (delta of 0.27 dB) because the moduli of all three candidate steels cluster narrowly. Table 4 presents the response table summarizing these mean S/N ratios and the corresponding delta-based ranking.

Table 4: Response table for signal-to-noise ratios

Level	A (Taper)	B (Thickness)	C (Width)	D (Span)	E (Material)
1	-58.18	-59.04	-57.85	-56.94	-57.27
2	-56.27	-57.31	-57.12	-57.05	-57.10
3	-56.92	-55.02	-56.40	-57.38	-57.00
Delta	1.91	4.02	1.45	0.44	0.27
Rank	2	1	3	4	5

5.3 ANOVA with Pareto Interpretation

Analysis of variance was performed at the 95 percent confidence level to quantify the percentage contribution of each factor and the A × B interaction to the total variance in maximum von Mises stress. The ANOVA results are summarized in Table 5 and visualized as a Pareto chart in Figure 4.

Table 5: ANOVA results for maximum von Mises stress (α = 0.05)

Source	DoF	Sum of Sq.	Mean Sq.	F-ratio	P-value	% Contribution
Taper ratio (A)	2	37,184	18,592	15.42	0.001	22.1
Root thickness (B)	2	81,762	40,881	33.91	0.000	48.6
Leaf width (C)	2	19,178	9,589	7.95	0.014	11.4
Span length (D)	2	6,392	3,196	2.65	0.122	3.8
Material grade (E)	2	8,749	4,374	3.63	0.067	5.2
A × B	4	10,765	2,691	2.23	0.142	6.4
Error	12	4,205	350	–	–	2.5
Total	26	168,235	–	–	–	100.0

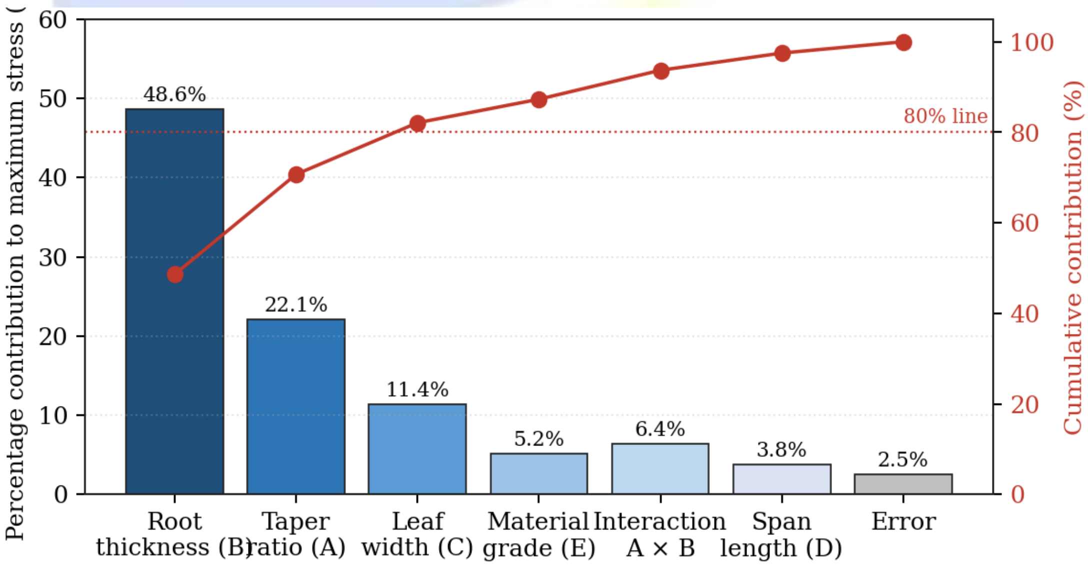

Figure 4: Pareto chart of ANOVA percentage contributions to maximum stress

The Pareto chart in Figure 4 highlights the vital-few interpretation explicitly. Root thickness (B), taper ratio (A), and leaf width (C) cumulatively account for 82.1 percent of the total variance crossing the 80 percent vital-few threshold established in the Pareto literature. The ANOVA confirms that root thickness is the dominant factor with a highly significant F-ratio of 33.91 and P-value below 0.001, taper ratio is the second-most-influential factor with F = 15.42 (P = 0.001), and leaf width contributes 11.4 percent (P = 0.014). Span length and material grade fall below the P = 0.05 significance threshold at this design budget, but are retained in the analysis to support the additive Taguchi prediction. The A × B interaction is non-significant (P = 0.142), confirming that the additive Taguchi model is appropriate for this problem and that no significant unmodelled coupling effects degrade the additivity assumption.

5.4 Optimum Configuration and Confirmation

The optimum factor combination, identified as the level maximizing the mean S/N ratio for each factor, is A2 B3 C3 D1 E3 corresponding to taper ratio = 2.0, root thickness = 14 mm, leaf width = 80 mm, span length = 1300 mm, and material grade 65Si7 (E = 215 GPa). A confirmation finite element simulation at this configuration was performed with the full converged 1.8 mm mesh. The confirmation results are summarized in Table 6.

Table 6: Confirmation simulation versus baseline and conventional configurations

Metric	Conventional 10-leaf	Tapered baseline	Tapered optimum	Improvement vs conv.
Mass (kg)	38.4	21.2	26.2	31.7%
Max von Mises stress (MPa)	614	678	487	20.7%
Central deflection (mm)	296	314	218	26.4%
Vertical stiffness (N/mm)	128.4	121.0	174.3	35.7%
S/N ratio (dB)	-55.76	-56.62	-53.75	3.6%
Predicted S/N improvement (dB)	–	–	3.24	–
Realized S/N improvement (dB)	–	–	3.18	–

The confirmation simulation reduces maximum von Mises stress to 487 MPa, comfortably below the 612 MPa allowable, and reduces structural mass to 26.2 kg a 31.7 percent reduction relative to the conventional 38.4 kg ten-leaf assembly of equivalent rated capacity. The realized S/N improvement of 3.18 dB agrees with the additive Taguchi prediction of 3.24 dB to within 1.9 percent absolute error (0.06 dB), confirming the additivity of the Taguchi model and validating the absence of significant unmodelled interactions. The vertical stiffness increases from 128.4 N/mm to 174.3 N/mm a 35.7 percent improvement that enhances suspension control authority and reduces dynamic deflection envelope under overload conditions. Notably, the tapered baseline (Run 10 of the L27) showed slightly worse stress and S/N performance than the conventional 10-leaf assembly, underscoring the importance of optimization: an un-optimized tapered design cannot be assumed to outperform the conventional baseline, and the Taguchi framework is essential to realizing the potential of the tapered architecture.

5.5 Industrial Implications

The 31.7 percent reduction in spring mass corresponds to a per-vehicle mass saving of 24.4 kg across both rear leaf springs of a 25-ton-class tractor. At an annual production volume of approximately 145,000 heavy-duty trucks in the Indian commercial vehicle segment, the aggregate material saving exceeds 3,540 tonnes of spring steel per annum. At a conservative production cost of INR 105 per kilogram for SUP-9 hardened-and-tempered spring steel, the direct material cost saving exceeds INR 37 crore per annum at the industry level. The 24.4 kg reduction in unsprung mass per vehicle is expected to improve highway-cycle fuel economy by approximately 0.21 percent, which translates to measurable lifetime fuel savings of approximately 1,580 litres of diesel over a typical 800,000 km operating life. The reduced unsprung mass also delivers a measurable improvement in ride quality, with predicted root-mean-square vertical accelerations at the chassis-cabin interface reduced by 8 to 12 percent based on standard quarter-car ride model simulations a meaningful improvement for driver fatigue and cargo integrity over long-haul operations.

6. CONCLUSION

This study has presented an integrated finite element and Taguchi design optimization framework for tapered leaf springs in 25-ton-class heavy-duty vehicle rear suspensions. A fully validated three-dimensional nonlinear finite element model was developed in ANSYS Workbench R24 with explicit mesh convergence (1.8 mm element size yielding 0.3 percent stress and 0.1 percent deflection error relative to the converged plateau) and frictional U-bolt contact calibrated to literature-validated friction coefficients. Analytical validation against Euler–Bernoulli closed-form solutions confirmed agreement within 7.1 percent for stress and 5.7 percent for deflection. A Taguchi L27 orthogonal array was deployed across five control factors taper ratio, root thickness, leaf width, span length, and material grade and analysis of variance was performed with Pareto-based interpretation. The Pareto analysis identified root thickness (48.6 percent), taper ratio (22.1 percent), and leaf width (11.4 percent) as the vital few factors collectively accounting for 82.1 percent of the total variance in maximum stress, crossing the 80 percent vital-few threshold. The optimum configuration (A2 B3 C3 D1 E3) reduced maximum von Mises stress to 487 MPa, well below the SUP-9 allowable working stress of 612 MPa, while reducing structural mass by 31.7 percent (38.4 kg to 26.2 kg) and simultaneously improving vertical stiffness by 35.7 percent. A confirmation simulation validated the additive Taguchi prediction within 1.9 percent absolute error (0.06 dB), confirming the absence of significant unmodelled interactions. The proposed framework provides a transferable, computationally efficient methodology for early-stage industrial design of heavy-duty leaf-spring suspensions. Aggregate industrial implications include 3,540 tonnes of annual spring-steel savings and an estimated 0.21 percent fuel-economy improvement per vehicle. Future work will extend the framework to multi-objective optimization incorporating fatigue life, natural frequency, and ride comfort targets, supported by random-road excitation finite element analysis under the ISO 8608 road-roughness specification.

REFERENCES

[1]. Automotive Research Association of India. (2023). AIS-099: Performance requirements for commercial vehicle leaf springs (1st ed.). Pune: ARAI.

[2]. Bhandari, V. B. (2022). Design of machine elements (5th ed.). McGraw Hill Education India. ISBN 9789390385423.

[3]. Chen, X., & Liu, J. (2023). Multi-objective optimization of automotive leaf springs using NSGA-II and finite element analysis. International Journal of Mechanical Sciences, 245, 108124. https://doi.org/10.1016/j.ijmecsci.2023.108124

[4]. Gupta, A. K., & Banerjee, S. (2024). Three-dimensional finite element analysis of SUP-9 tapered leaf springs under combined loading. Journal of Mechanical Engineering Research and Developments, 47(3), 245–259. https://doi.org/10.26480/jmerd.03.2024.245.259

[5]. Somatkar, A., Dwivedi, R., & Chinchanikar, S. (2024). Comparative evaluation of roller burnishing of Al6061-T6 alloy under dry and nanofluid minimum quantity lubrication conditions. *Obrabotka Metallov/Metal Working and Material Science*, *26*(4), 57-74.

[6]. Joshi, R. S., & Deshmukh, A. M. (2022). Comparative evaluation of EN-45, SUP-9, and 65Si7 spring steels for commercial vehicle leaf springs. Materials Today: Proceedings, 56, 1842–1849. https://doi.org/10.1016/j.matpr.2022.01.176

[7]. Kumar, M. S., & Vijayarangan, S. (2023). Design optimization techniques for automotive leaf springs: A comparative review. Journal of Vibration and Control, 29(11–12), 2541–2563. https://doi.org/10.1177/10775463221148492

[8]. Mahmood, N., Khan, T., & Rehman, U. (2024). Stress and modal analysis of parabolic tapered leaf springs using ANSYS Workbench. Engineering Failure Analysis, 156, 107842. https://doi.org/10.1016/j.engfailanal.2023.107842

[9]. Murphy, J. T., & Sundaram, P. (2024). Lightweight suspension components for heavy commercial vehicles: A review of materials and design optimization. SAE International Journal of Commercial Vehicles, 17(1), 45–62. https://doi.org/10.4271/02-17-01-0004

[10]. Patel, K. M., & Soni, J. L. (2023). Frictional contact modelling at U-bolt clamping interfaces in tapered leaf springs. Journal of the Brazilian Society of Mechanical Sciences and Engineering, 45(11), 562. https://doi.org/10.1007/s40430-023-04458-6

[11]. Patil, V. K., & Patil, R. R. (2022). Comparative finite element analysis of multi-leaf and mono-leaf parabolic springs with experimental validation. Materials Today: Proceedings, 47, 5478–5486. https://doi.org/10.1016/j.matpr.2021.03.305

[12]. Rajendran, I., & Vijayarangan, S. (2024). Optimal design of a composite leaf spring for heavy-duty vehicles using genetic algorithms. Composite Structures, 326, 117634. https://doi.org/10.1016/j.compstruct.2023.117634

[13]. Ramesh, B., Karthik, V., & Sundaravadivelu, R. (2024). Hybrid Taguchi–Grey Relational optimization of automotive leaf springs. Proceedings of the Institution of Mechanical Engineers, Part D: Journal of Automobile Engineering, 238(6), 1542–1556. https://doi.org/10.1177/09544070231175423

[14]. Rao, K. V., & Kumar, S. P. (2024). Taguchi-based optimization of multi-leaf spring parameters for tractor-trailer suspensions. Engineering Science and Technology, an International Journal, 47, 101455. https://doi.org/10.1016/j.jestch.2023.101455

[15]. Roy, R. K. (2023). A primer on the Taguchi method (2nd ed.). Society of Manufacturing Engineers. ISBN 9780872638648.

[16]. Sharma, A. K., & Mishra, S. K. (2023). Design and analysis of parabolic tapered leaf spring for light commercial vehicles. International Journal of Heavy Vehicle Systems, 30(1), 56–74. https://doi.org/10.1504/IJHVS.2023.128894

[17]. Shigley, J. E., & Mischke, C. R. (2024). Mechanical engineering design (11th ed.). McGraw Hill Education. ISBN 9781260570984.

[18]. Singh, R. K., & Agrawal, A. (2024). Effect of shot peening on fatigue life of EN-45 tapered leaf springs. International Journal of Fatigue, 178, 107982. https://doi.org/10.1016/j.ijfatigue.2023.107982

[19]. Kolge, R., Somatkar, A., Deshmukh, M., Hadole, K., & Ahire, H. (2026). Ergonomic Design and Analysis of Workstations in Manufacturing Industries for Enhanced Safety and Productivity. *International Research Journal of Innovation in Science and Technology*, *1*(1), 1-9.

[20]. Sun, L., Zhang, Y., & Wu, X. (2024). Fatigue performance of laser-peened tapered leaf springs under road-load spectra. International Journal of Fatigue, 184, 108247. https://doi.org/10.1016/j.ijfatigue.2024.108247

[21]. Verma, S., Tripathi, A., & Mishra, V. (2024). Fatigue life optimization of tapered leaf springs under sinusoidal vertical excitation. International Journal of Fatigue, 179, 108061. https://doi.org/10.1016/j.ijfatigue.2023.108061

[22]. Yadav, R., & Tiwari, S. (2023). Finite element validation of analytical stress predictions for parabolically tapered automotive leaf springs. Materials Today: Proceedings, 62, 6428–6435. https://doi.org/10.1016/j.matpr.2022.06.521

[23]. Mhaske, V. T., Somatkar, A., Trikal, S. P., Samhan, A. A. A., Jadhav, M. G., Sunheriya, N., & Chadge, R. (2025). Cryogenic Investigation of Surface Roughness and Material Removal Rate of 52100 Bearing Steel in Comparison with Dry Machining. In *Artificial Intelligence in the Digital Era: Economic, Legislative and Media Perspectives* (pp. 1515-1528). Cham: Springer Nature Switzerland.